Volume 1 | Number 1 | Jan 2013 | Pages 1–100

Dalton Transactions

An international journal of inorganic chemistry
www.rsc.org/dalton

ROYAL SOCIETY OF CHEMISTRY

This is an *Accepted Manuscript*, which has been through the Royal Society of Chemistry peer review process and has been accepted for publication.

Accepted Manuscripts are published online shortly after acceptance, before technical editing, formatting and proof reading. Using this free service, authors can make their results available to the community, in citable form, before we publish the edited article. We will replace this *Accepted Manuscript* with the edited and formatted *Advance Article* as soon as it is available.

You can find more information about *Accepted Manuscripts* in the **Information for Authors**.

Please note that technical editing may introduce minor changes to the text and/or graphics, which may alter content. The journal's standard **Terms & Conditions** and the **Ethical guidelines** still apply. In no event shall the Royal Society of Chemistry be held responsible for any errors or omissions in this *Accepted Manuscript* or any consequences arising from the use of any information it contains.

Assembly of Heterobimetallic Ni^{II}-Ln^{III}(Ln^{III} = Dy^{III}, Tb^{III},Gd^{III},Ho^{III}, Er^{III}, Y^{III}) Complexes Using a Ferrocene Ligand: Slow Relaxation of the Magnetization in Dy^{III,} Tb^{III} and Ho^{III} Analogues

Amit Chakraborty,[a] Prasenjit Bag,[a] Eric Rivière,[b] Talal Mallah,[b] Vadapalli Chandrasekhar[a,c]

[a]Department of Chemistry, Indian Institute of Technology Kanpur, Kanpur-208016, India

[b]Institut de Chimie Moleculaire et Mate riaux d'Orsay, Universite Paris-Sud 11, F-91405, Orsay, France

[c]National Institute of Science Education and Research, Institute of Physics Campus, Sachivalaya Marg, Sainik School Road, Bhubaneshwar-751 005, Odisha, India

Abstract

A family of dinuclear 3d-4f heterobimetallic complexes [LNi(H$_2$O)(μ-OAc)Ln(NO$_3$)$_2$]· CH$_3$CN; {(Ln= Dy^{III}(**1**), Tb^{III}(**2**), Ho^{III}(**3**), Gd^{III}(**4**), Er^{III}(**5**), Y^{III}(**6**) } have been synthesized by utilizing a ferrocene-based, dual compartmental ligand H$_2$L. **1-6** are isostructural which crystallize in the triclinic (*P*-1) space group. In these complexes Ni^{II} is present in the inner coordination sphere of the dianionic [L]$^{2-}$ ligand; Ln^{III} is encapsulated in the outer coordination pocket. Ni^{II} shows a 2N, 4O coordination environment in a distorted octahedral geometry, while the Ln^{III} ion possesses a 9O coordination environment in a distorted tricapped trigonal prismatic geometry. ESI-MS studies suggest that the structural integrity of **1-6** is retained in solution. Electrochemical studies reveal that these complexes show a reversible one-electron response typical for the ferrocene motif along with an irreversible one-electron oxidation involving the Ni^{II}/Ni^{III} couple. Magnetic studies revealed the presence of ferromagnetic exchange coupling between Ni^{II} and Ln^{III} centers as shown by the increase of χ_MT value upon cooling below the 50 K for compounds **1**, **2**, **4** and **5**. Further, dynamic magnetic susceptibility measurements (**1-3**) confirm the absence of an out-of-phase (χ'') signal at zero *dc* fields. However, when these measurements were carried out at 1000 Oe *dc* field the χ'' signal was observed, although a maxima could not be detected up to 2 K.

KEYWORDS: Ferrocene, compartmental ligand, heterometallic complexes, cyclic voltammetry, magnetism, *ac* susceptibility studies.

.

Introduction

Recently there has been considerable research activity in the area of heterometallic 3d/4f complexes.[1,2] This interest is mainly motivated by the extremely interesting magnetic properties of such complexes which is the result of the magnetic interactions between the 3d and 4f metal ions as well as the intrinsic magnetic anisotropy of these ions. Many 3d/4f complexes, particularly those that contain Cu(II),[3] Mn(III)[4] or Fe(II/III)[5] have shown single-molecule magnet (SMM) properties. In general, SMM behavior is exhibited by molecules that possess a large ground state spin and a large uni-axial magnetic anisotropy.[6] In view of the fact that Co^{II} and Ni^{II} also possess significant magnetic anisotropy[7], in recent years, there have been efforts to incorporate these metal ions in 3d/4f complex systems.[8,9] However, the number of such examples are still not very large.

We have been utilizing phosphorus-supported ligands such as $SP[N(Me)N=CH-C_6H_3-2-OH-3-OMe]_3$[10] and $[\{N_2P_2(O_2C_{12}H_8)_2\}\{NP\{N(CH_3)N=CH-C_6H_3-(2-OH)(3-OCH_3)\}_2\}]$[11] to prepare heterometallic tri- and dinuclear 3d/4f complexes some of which were shown to possess SMM behavior at low temperatures.[10] In order to expand the repertoire of the ligand systems for preparing SMMs, we looked at ferrocene as a possible scaffold particularly because of the thermal stability of this compound, its solubility in common organic solvents, as well as the ease of modifying its cyclopentadienyl skeleton. Indeed, in recent years ferrocene-based ligands are being extensively investigated, particularly in regard to generating novel catalytic systems for C-C bond formation reactions.[12] Compartmental ligands have been utilized previously for the preparation of heterometallic complexes.[13] We have recently designed a ferrocene-based compartmental ligand, H_2L, which was used for assembling heterometallic 3d-4f metal complexes containing Zn^{II} ion.[14] In view of the interest in Ni^{II}/4f complexes we have utilized

H_2L for the assembly of dinuclear Ni^{II}/Ln^{III} complexes. Accordingly, herein, we report the synthesis, structural characterization and magnetic properties of $[LNi(H_2O)(\mu\text{-}OAc)Dy(NO_3)_2.$ $CH_3CN](\mathbf{1})$, $[LNi(H_2O)(\mu\text{-}OAc)Tb(NO_3)_2.$ $CH_3CN](\mathbf{2})$, $[LNi(H_2O)(\mu\text{-}OAc)Ho(NO_3)_2.$ $CH_3CN](\mathbf{3})$, $[LNi(H_2O)(\mu\text{-}OAc)Gd(NO_3)_2.$ $CH_3CN](\mathbf{4})$, $[LNi(H_2O)(\mu\text{-}OAc)Er(NO_3)_2.$ $CH_3CN](\mathbf{5})$, $[LNi(H_2O)(\mu\text{-}OAc)Y(NO_3)_2. CH_3CN](\mathbf{6})$.

Experimental section

Reagents and General Procedures

All the solvents were purified by adopting standard procedures.[15] Ferrocene (Sigma-Aldrich, USA), acetyl chloride (Spectrochem, Mumbai), aluminum chloride, hydrazine hydrate, *o*-vanillin (2-hydroxy-3-methoxybenzaldehyde), $Ni(OAc)_2 \cdot 4H_2O$, $Ln(NO_3)_3 \cdot xH_2O$ (Ln^{III} = Dy^{III}, Tb^{III}, Gd^{III}, Ho^{III}, Er^{III}, Y^{III}) were used as purchased ((SIGMA-ALDRICH, USA)). Diacetylferrocene and 1,1′-diacetylferrocene dihydrazone were synthesized and purified according to reported procedures.[16, 17]

Instrumentation

Melting points were measured using a JSGW melting point apparatus. ESI-MS spectra were recorded on a Micromass Quattro II triple quadrupole mass spectrometer. ^1H NMR spectra were obtained on a JEOL-JNM Lambda 400 model and a JEOL-DELTA 2500 model NMR spectrometer using $CDCl_3$ as the solvent and tetramethylsilane as the reference. NMR data are reported in ppm. Elemental analysis were carried out on fully dried samples using a Thermoquest CE Instruments CHNS-O, EA/110 model. IR spectra were recorded as KBr pellets in the range of 4000−400 cm^{-1} on a Bruker FT-IR Vector 22 model. UV−Vis spectra were recorded on a

Perkin-Elmer Lambda 20 UV−Vis spectrometer in ~ 10^{-5} M chloroform solutions. Details are given in the ESI .

Cyclic voltammetric studies were performed on a BAS Epsilon electrochemical workstation using a glassy carbon working electrode, an Ag/AgCl reference electrode (3 M NaCl), and a platinum-wire counter electrode. All measurements were performed using 1 mM concentration of the complexes in the presence of 0.1 M TBAP in dry dichloromethane.

X-Ray diffraction

Single-crystal X-ray diffraction studies were performed on a Bruker SMART CCD diffractometer (MoKα radiation, λ = 0.71073 Å).The SMART program was used for collecting frames of data,[18a] indexing reflections, and determining lattice parameters and SAINT PLUS[18b] has been used to obtain integration of the intensity of reflections and scaling and SADABS[18c] for absorption correction, and SHELXTL[18d] for space group and structure determination and least-squares refinements on F^2. All the structures were solved by direct methods using the program SHELXS-97[18e] and then refined by full-matrix least-squares methods against F^2 with SHELXL-97. All the non-hydrogen atoms were refined with anisotropic displacement parameters. All the hydrogen atoms were fixed at calculated positions and their positions were refined by a riding model. The crystallographic figures were generated using Diamond 3.1e software.[18f] The crystal data and the cell parameters for compounds **1**-**6** are summarized in Table 1 and Table 2. CCDC reference numbers for **1**-**6** are 993944-993949 respectively.

Table 1. Crystal and Refinement Data for **1-3.**

Compound	1	2	3
Formula	$C_{34}H_{36}DyFeN_7NiO_{13}$	$C_{34}H_{36}TbFeN_7NiO_{13}$	$C_{34}H_{36}HoFeN_7NiO_{13}$
M w/g	1027.74	1024.17	1030.18
Crystal system	Triclinic	Triclinic	Triclinic
Space group	P -1	P -1	P-1
a/Å	12.208(5)	12.293(5)	12.313(4)
b/Å	12.313(5)	12.354(5)	12.378(4)
c/Å	12.459(5)	12.498(5	12.530(4)
$\alpha(°)$	97.914(5)	98.128(5)	98.030(6)
β (°)	92.016(5)	91.977(5)	91.972(6)
$\gamma(°)$	99.686(5)	99.904(5)	100.182(6)
V/Å^3	1825.3(13)	1847.6(13)	1857.7(11)
Z	2	2	2
ρ_c/g cm^{-3}	1.870	1.841	1.842
μ /mm^{-1}	3.006	2.861	3.072
$F(000)$	1026	1024.0	1028
Crystal size (mm^3)	0.10 x 0.09 x 0.08	0.11 x 0.10 x 0.09	.07 x .06 x .05
θ range (°)	2.19 to 25.50°	1.68 to 25.50°	1.68 to 27.00°.
Limiting indices	-14<=h<=14, -7<=k<=14, -14<=l<=15	-14<=h<=14, -14<=k<=14, -15<=l<=9	-15<=h<=15, -15<=k<=15, -16<=l<=16
Reflns collected	9397	9912	29219
Indreflns	6577 [R(int) = 0.0439]	6705 [R(int) = 0.0304]	8042 [R(int) = 0.0306]
Completeness to θ (%)	96.8 %	97.5 %	99.3 %

Refinement method	Full-matrix least-squares on F^2	Full-matrix least-squares on F^2	Full-matrix least-squares on F^2
Data/Restraints/Params	6577 / 20 / 522	6705 / 14 / 522	8042 / 0 / 528
Goodness-of-fit on F^2	1.072	1.082	1.076
Final R indices [$I > 2\theta(I)$]	$R1 = 0.0688$, $wR2 = 0.1598$	$R1 = 0.0513$, $wR2 = 0.0995$	$R1 = 0.0290$, $wR2 = 0.0584$
R indices (all data)	$R1 = 0.1035$, $wR2 = 0.1874$	$R1 = 0.0739$, $wR2 = 0.1256$	$R1 = 0.0378$, $wR2 = 0.0648$
Largest diff. peak and hole(e.Å^{-3})	3.126 and -1.678	1.593 and -1.013	1.244 and -0.900

Table 2. Crystal and Refinement Data for **4- 6.**

Compound	4	5	6
Formula	$C_{34}H_{36}GdFeN_7NiO_{13}$	$C_{34}H_{36}ErFeN_7NiO_{13}$	$C_{34} H_{36} Fe N_7 Ni O_{13} Y$
M w/g	1022.49	1032.50	955.16
Crystal system	Triclinic	Triclinic	Triclinic
Space group	P -1	P -1	P -1
a/Å	12.377(5)	12.262(5)	12.238(5)
b/Å	12.390(5)	12.365(5)	12.345(5)
c/Å	12.485(5)	12.503(5)	12.486(5)
α(°)	91.923(5)	98.072(5)	98.068(5)
β (°)	98.147(5)	92.025(5)	92.083(5)
γ(°)	100.163(5)	100.116(5)	99.950(5)
V/Å^3	1862.2(13)	1844.2(13)	1836.0(13)
Z	2	2	2
ρ_c /g cm^{-3}	1.824	1.859	1.728
μ /mm^{-1}	2.721	3.225	2.542

F(000)	1023.44	1030.0	974.0
Crystal size (mm^3)	0.11 x 0.10 x 0.09	0.09 x 0.08 x 0.07	0.15 x 0.13 x 0.11
θ range (deg)	2.15 to 25.50°.	2.16 to 25.50°.	2.17 to 25.50°
Limiting indices	-14<=h<=13, -12<=k<=14, -15<=l<=15	-14<=h<=14, -14<=k<=14, -11<=l<=15	-12<=h<=14, -14<=k<=14, -15<=l<=15
Reflns collected	9993	9813	12772
Indreflns	6767 [R(int) = 0.0260]	6710 [R(int) = 0.0325]	6789 [R(int) = 0.0242]
Completeness to θ (%)	97.9 %	97.8 %	99.5 %
Refinement method	Full-matrix least-squares on F^2	Full-matrix least-squares on F^2	Full-matrix least-squares on F^2
Data/Restraints/Params	6767 / 2 / 504	6710 / 3 / 523	6789 / 0 / 523
Goodness-of-fit on F^2	1.100	1.025	1.049
Final R indices [$I > 2\theta(I)$]	*R1* = 0.0497, *wR2* = 0.1128	*R1* = 0.0534, *wR2* = 0.1302	*R1* = 0.0375, *wR2* = 0.0822
R indices (all data)	*R1* = 0.0643, *wR2* = 0.1206	*R1* = 0.0766, *wR2* = 0.1579	*R1* = 0.0485, *wR2* = 0.0867
Largest diff. peak and hole(e.Å^{-3})	1.322 and -1.529	2.346 and -0.939	1.032 and -0.614

Synthesis

Preparation of heterobimetallic complexes 1-6

The following general procedure was applied to prepare the metal complexes **1-6**. Ligand H$_2$L[14] was dissolved in a chloroform/methanol mixture (30 mL, v/v, 1:1). Triethylamine (0.05mL, 35.5 mg, 0.352 mmol) was added to this solution and stirred for a few minutes. To this mixture,

$Ni(OAc)_2 \cdot 4H_2O$ was added all at once, followed by $Ln(NO_3)_3 \cdot xH_2O$ (Ln^{III} = Dy^{III}, Tb^{III}, Gd^{III}, Ho^{III}, Er^{III}, Y^{III}). After this, the reaction mixture was heated under reflux for 2h and then allowed to come to room temperature. Solvent was removed from the reaction mixture, under vacuum, affording a solid which was washed with diethyl ether (10 mL). The solid residue was dissolved in chloroform/acetonitrile mixture (5mL/10mL) and kept for crystallization at 5 ºC temperature. X-ray quality crystals were obtained in about 2-3 weeks. The details regarding quantities and yields for each of the complexes are given below.

[LNi(H₂O)(μ-OAc)Dy(NO₃)₂] CH₃CN (1)

Quantities: $Ni(OAc)_2 \cdot 4H_2O$(44.0mg, 0.178 mmol), $Dy(NO_3)_3 \cdot 5H_2O$ (77.5mg, 0.176mmol), H_2L (100.0mg, 0.176mmol). Yield: 70mg, 40.6%. Mp: > 250ºC (d), IR (KBr, v/cm^{-1}): 3252(m, br), 2946(w), 2945(w), 1609(s), 1574(s), 1469(s), 1301(s), 1220(s), 739(s). Anal. Calcd. for $C_{34}H_{36}DyFeN_7NiO_{13}$ (1027.74): C, 39.73; H, 3.53; N, 9.54. Found: C, 39.68; H, 3.50; N, 9.65. ESI-MS (positive ion mode) in CH_3OH: m/z 909.9$[LNiDy(NO_3)_2]^+$.

[LNi(H₂O)(μ-OAc)Tb(NO₃)₂] CH₃CN (2)

Quantities: $Ni(OAc)_2 \cdot 4H_2O$ (44.0mg, 0.176mmol), $Tb(NO_3)_3 \cdot 5H_2O$ (76.5mg, 0.176mmol), H_2L (100.0mg, 0.176mmol). Yield: 65mg, 37.8%. Mp: > 250ºC(d), IR (KBr, v/cm^{-1}): 3250 (m, br), 2947 (w), 1609 (s), 1468 (s), 1220 (s), 740 (s). Anal. Calcd. for $C_{34}H_{36}TbFeN_7NiO_{13}$ (1024.17): C, 39.87; H, 3.54; N, 9.57. Found: C, 39.65; H, 3.48; N, 9.62. ESI-MS (positive ion mode) in CH_3OH: m/z 904.9$[LNiTb(NO_3)_2]^+$.

[LNi(H₂O)(μ-OAc)Ho(NO₃)₂] CH₃CN (3)

Quantities: Ni(OAc)$_2$·4H$_2$O(44.0mg, 0.176mmol), Ho(NO$_3$)$_3$·6H$_2$O (79.70mg, 0.176mmol), H$_2$L (100.0mg, 0.176mmol). Yield: 75mg, 43.7%. Mp: > 250°C(d), IR (KBr, v/cm^{-1}): 3250 (m, br), 2975 (m), 2677 (s), 2491 (w), 1609(s), 1470(s), 1435 (s), 743 (s). Anal. Calcd for C$_{34}$H$_{36}$HoFeN$_7$NiO$_{13}$ (1030.18): C, 39.64; H, 3.52; N, 9.52. Found:, 39.70; H, 3.44; N, 9.60. ESI-MS (positive ion mode) in CH$_3$OH: m/z 877.0 [LNiμ-OAc)Ho + OMe]$^+$.

[LNi(H$_2$O)(μ-OAc)Gd(NO$_3$)$_2$. CH$_3$CN](4)

Quantities: Ni(OAc)$_2$·4H$_2$O (44.0 mg, 0.176 mmol), Gd(NO$_3$)$_3$·5H$_2$O (78.02 mg, 0.176 mmol), H$_2$L (100.0 mg, 0.176 mmol).Yield: 60 mg, 34.6%. Mp: > 250°C(d). IR (KBr, v/cm^{-1}): 3358 (m, br), 2939 (m), 2677 (m), 1608(s), 1468 (s), 1220 (s), 740(s). Anal. Calcd. For C$_{34}$H$_{36}$GdFeN$_7$NiO$_{13}$ (1022.49): C, 39.94; H, 3.55;N, 9.59. Found: C, 39.86; H, 3.65;N, 9.57. ESI-MS (positive ion mode) in CH$_3$OH: m/z 903.9[LNiGd(NO$_3$)$_2$]$^+$.

[LNi(H$_2$O)(μ-OAc)Er(NO$_3$)$_2$. CH$_3$CN](5)

Quantities: Ni(OAc)$_2$·4H$_2$O(44.0mg, 0.176mmol), Er(NO$_3$)$_3$·5H$_2$O (77.6mg, 0.176mmol), H$_2$L (100.0mg, 0.176mmol). Yield: 65mg, 37.6%. Mp: > 250°C (d). IR (KBr, v/cm^{-1}): 3375 (m, br), 2942 (w), 1609 (s), 1471 (s), 1302 (s), 1220 (s), 744 (s). Anal. Calcd. For C$_{34}$H$_{36}$ErFeN$_7$NiO$_{13}$ (1032.50): C, 39.55; H, 3.51; N, 9.50. Found: C, 39.45; H, 3.53; N, 9.65. ESI-MS (positive ion mode) in CH$_3$OH: m/z 880.0 [LNi(μ-OAc)Er + OMe]$^+$.

[LNi(H$_2$O)(μ-OAc)Y(NO$_3$)$_2$. CH$_3$CN](6)

Quantities: Ni(OAc)$_2$·4H$_2$O (44.0 mg, 0.176 mmol), Y(NO$_3$)$_3$·6H$_2$O (68.00 mg, 0.177 mmol), H$_2$L (100.0 mg, 0.176 mmol).Yield: 50 mg, 31.1%. Mp: > 250°C(d). IR (KBr, v/cm^{-1}): 3419.69

(m, br), 2971.92 (m), 1620.21 (s), 1253.39 (s). Anal. Calcd. For $C_{34}H_{36}YFeN_7NiO_{13}$ (954.13): C, 42.80; H, 3.80; N, 10.28; Found: C, 42.72; H, 3.78; N, 10.35. ESI-MS (positive ion mode) in CH_3OH: m/z 801.0 $[LNi(\mu\text{-}OAc)Y + OMe]^+$.

Results and discussion

Synthetic aspects

Site-specific coordination ligands, with different types of metal-binding sites, are an excellent choice for assembling 3d–4f heterometallic complexes. The ligand H_2L built on a ferrocene platform, utilizing both its cyclopentadienyl arms, possesses 6 coordination sites which can be partitioned into two coordination pockets (Scheme 1).
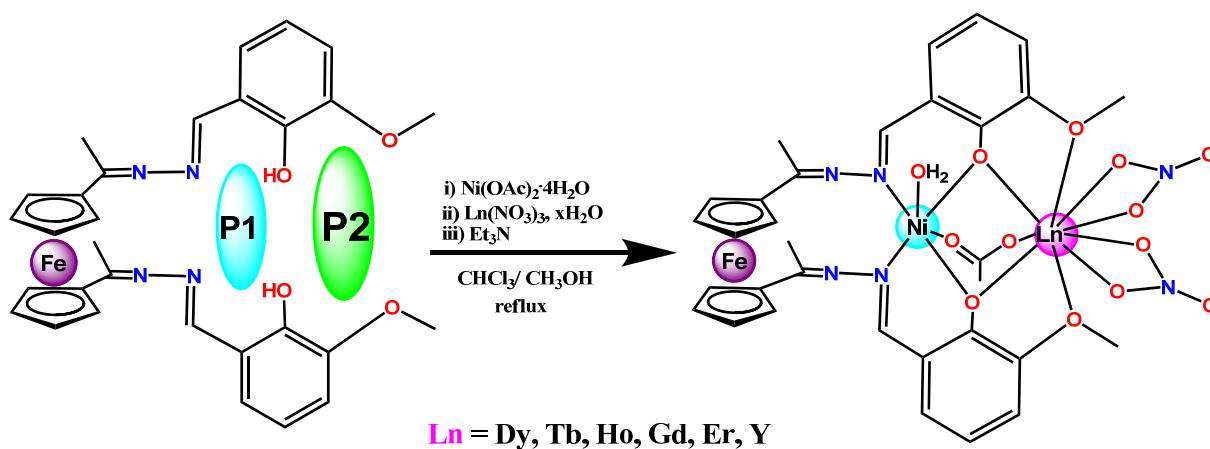
Scheme 1. Synthesis of the heterometallic $Ni^{II}/4f$ complexes **1-6.**

The inner pocket (P1) consists of two imine nitrogen and two strongly binding phenolateoxygen atoms (suitable for divalent transition metal ion), whereas the outer pocket (P2) contains two phenolate and two methoxy oxygen atoms (suitable for a lanthanide metal ion). Accordingly, a

one-pot synthesis, involving H_2L/triethylamine/Ni^{II} salt/Ln^{III} salt, afforded in excellent yields,

the heterometallic complexes $LNi(H_2O)(\mu\text{-OAc})Ln(NO_3)_2$ [Ln^{III} = Dy^{III} (**1**), Tb^{III} (**2**), Gd^{III} (**3**),

Ho^{III} (**4**), Er^{III} (**5**) and Y^{III}(**6**)]. These complexes are quite stable in solution also, as confirmed by

their ESI-MS (see Figure 1 and ESI). Thus, **1** reveals the presence of a peak at 909.98 of the

fragment corresponding to $[LNiDy(NO_3)_2]^+$ in its ESI-MS spectrum (Figure 1).

(a)   (b)
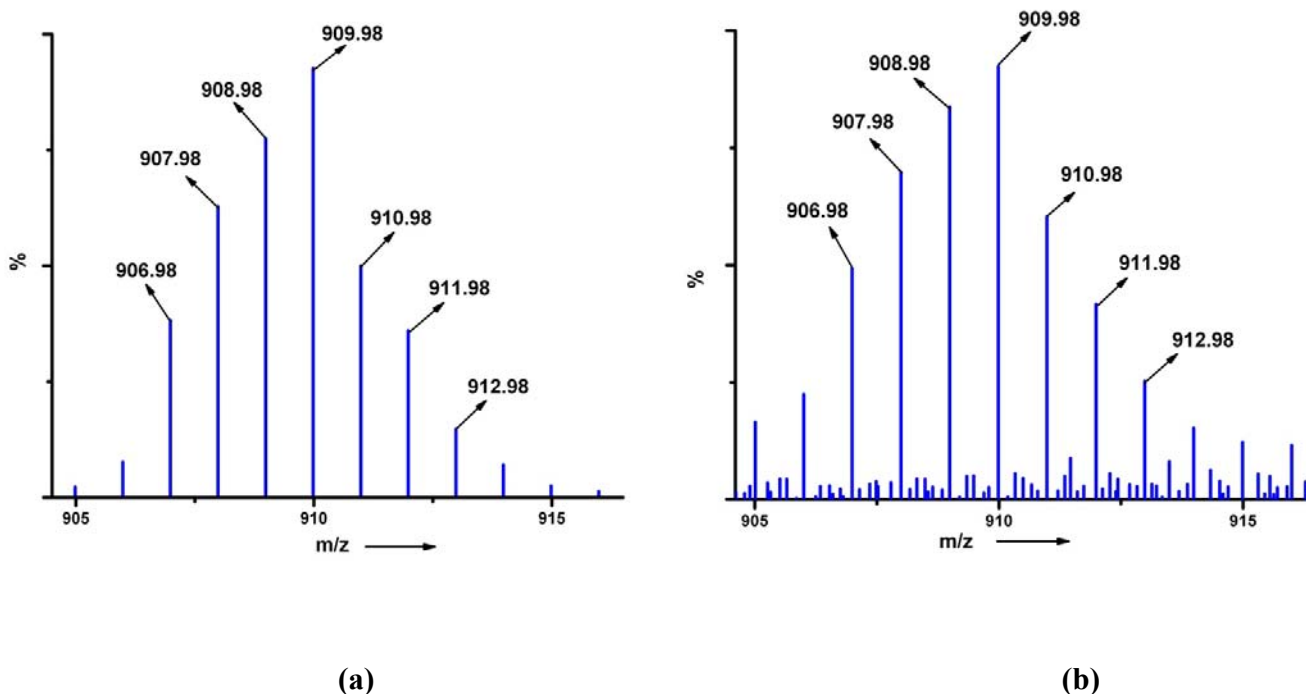
Figure 1. ESI-MS of **1** showing the fragment $[LNiDy(NO_3)_2]^+$ at m/z 909.98 (a) theoretical

simulation; (b) experimental spectrum.

X-ray crystal structures of 1-6.

The molecular structure of the heterometallic complexes LNi(H$_2$O)(μ-OAc)Ln(NO$_3$)$_2$(Ln^{III} = Dy^{III}, Tb^{III}, Gd^{III}, Ho^{III}, Er^{III}, Y^{III}) (**1-6**) were confirmed by X-ray crystallography. All the complexes crystallized in the triclinic *P*-1 space group and are isomorphs (containing the same solvent of crystallization). In all the complexes the asymmetric unit contains one full molecule. In view of the structural similarity of **1-6**, we have chosen LNi(H$_2$O)(μ-OAc)Dy(NO$_3$)$_2$(**1**) as a representative example for illustrating the structural features of these complexes. The structural details of other compounds are given in the ESI.

The molecular structure of **1** is given in Figure 2. Selected bond parameters of this complex are summarized in the caption of Figure 2. The formation of **1** involved, as anticipated, the selective binding of Ni^{II} in the coordination pocket 1 and that of Dy^{III} in the coordination pocket 2. The ligand H$_2$L binds to the metal ions in its de-protonated form, [L]$^{2-}$. Ni^{II} is six-coordinated (2N, 4O) in a distorted octahedral geometry (Figure 3). The two hydrazone nitrogen atoms [Ni(1)-N(2), 2.087(9) Å; Ni(1)-N(4), 2.117(8) Å] along with the two phenolate oxygen atoms [Ni(1)-O(1), 2.057(7) Å; Ni(1)-O(3), 2.034(7) Å] are present in the equatorial plane in a *cis* orientation. While one of the axial positions is taken up by a water molecule [Ni(1)-O(13), 2.073(8) Å] the other is occupied by an oxygen atom of a bridging acetate ligand [Ni(1)-O(5), 2.034(7) Å]. In contrast to Ni^{II}, Dy^{III} is selectively bound by the outer coordination pocket, P2, of the ligand [L]$^{2-}$. Dy^{III} is nine-coordinate, in a distorted tricapped trigonal prismatic geometry (Figure 3), contained in an all-oxygen environment (9O). The coordinating atoms involve the two phenolate oxygen atoms [Dy(1)-O(1), 2.317(7) Å; Dy(1)-O(3), 2.306(7) Å], the two methoxy oxygen atoms [Dy(1)-O(2), 2.603(8) Å; Dy(1)-O(4), 2.532(8) Å], two chelating nitrate ligands [Dy(1)-O(7), 2.440(9) Å; Dy(1)-O(8), 2.412(7) Å; Dy(1)-O(10), 2.518(7) Å; Dy(1)-O(11), 2.437(7) Å]

and a bridging acetate ligand [Dy(1)-O(6), 2.284(7) Å]. Dy^{III} and Ni^{II} are bridged to each other

by the phenolate oxygen atoms O3 and O1 as well as by the isobidentate acetate ligand (O5 and

O6). As a result of this cumulative coordination, Dy^{III} forms part of three 4-membered, two 5-

membered and two 6-membered rings, while Ni^{II} forms part of one 4-membered, four six-

membered and one 10-membered ring systems (ESI, Figure S16).The four- membered $NiDyO_2$

ring formed by phenolate oxygen bridges, is puckered, where O(1) and O(3) are displaced from

the mean plane by 0.21(1) Å and 0.25(1) Å respectively.
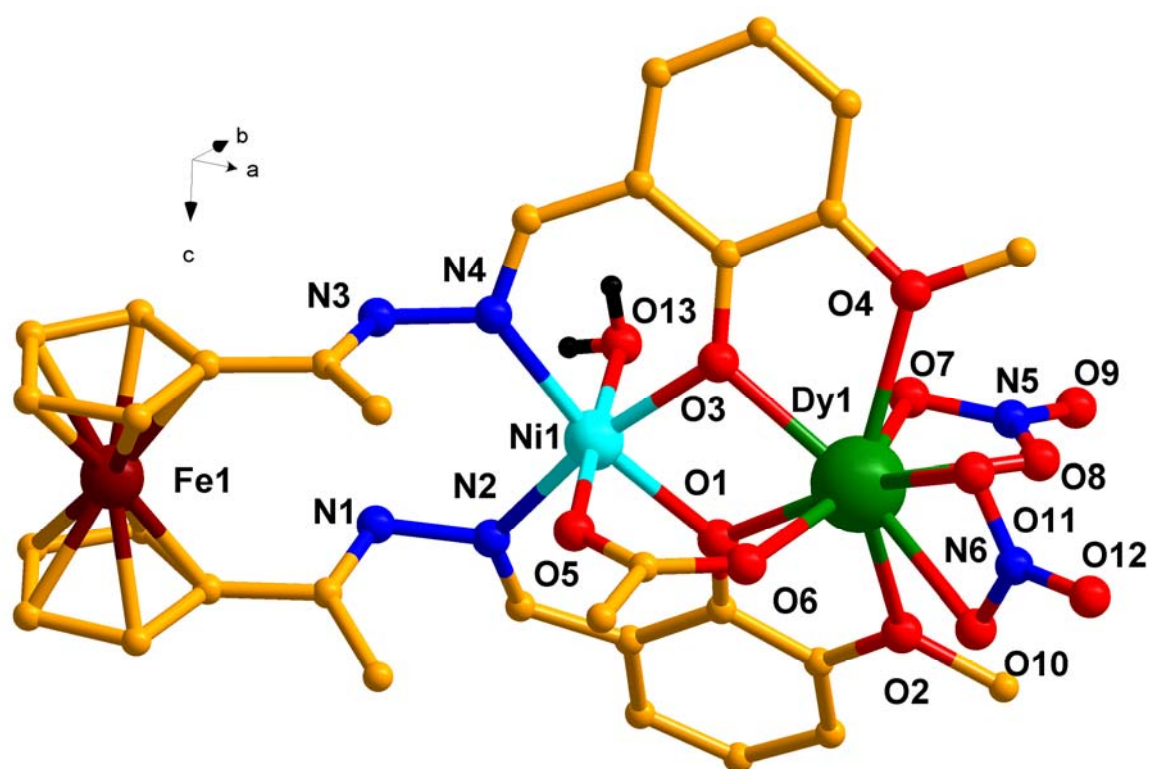
Figure 2. Molecular structure of **1**. Hydrogen atoms are omitted for clarity. Selected bond

distances (Å) : Dy(1)-O(1), 2.317(7); Dy(1)-O(2), 2.603(8); Dy(1)-O(3), 2.306(7); Dy(1)-O(4),

2.532(8); Dy(1)-O(6), 2.284(7); Dy(1)-O(7), 2.440(9); Dy(1)-O(8), 2.412(7); Dy(1)-O(10),

2.518(7); Dy(1)-O(11), 2.437(7); Ni(1)-N(2), 2.087(9); Ni(1)-N(4), 2.117(8); Ni(1)-O(1),

2.057(7); Ni(1)-O(3), 2.034(7); Ni(1)-O(5), 2.034(7); Ni(1)-O(13), 2.073(8); Bond angles(°):

O(1)-Dy(1)-O(2), 62.7(2); O(1)-Dy(1)- O(3), 70.6(3); O(3)-Dy(1)-O(4), 64.0(2); O(4)-Dy(1)-

O(2), 138.6(3); O(1)-Ni(1)-N(2), 87.1(3); O(3)-Ni(1)-N(4), 86.7(3); O(3)-Ni(1)-O(1), 81.6(3);

N(2)-Ni(1)-N(4), 104.6(3); Ni(1)-O(1)-Dy(1), 102.0(3); Ni(1)-O(3)-Dy(1), 103.1(3).
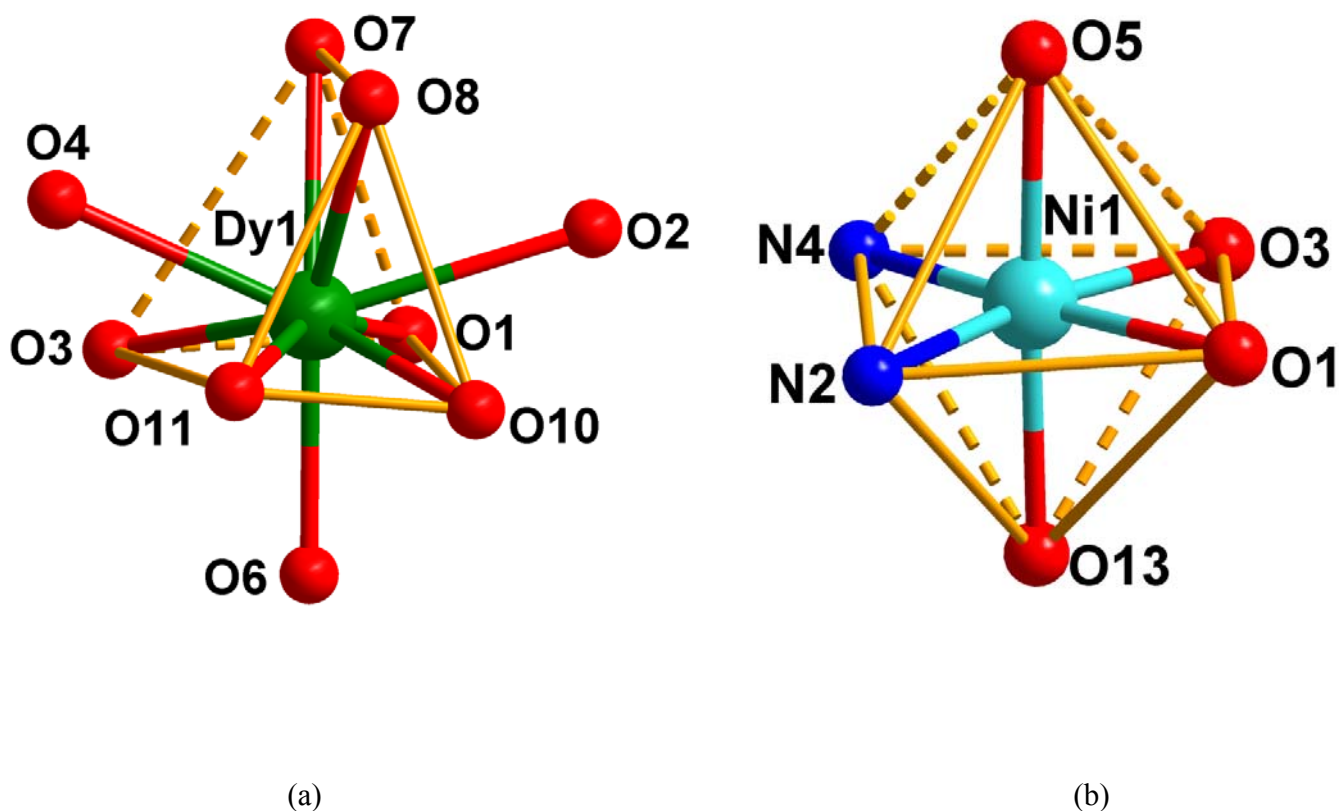

(a)   (b)

Figure 3. (a) Distortedtricappedtrigonal prismatic coordination environment around Dy(III), (b)

octahedral coordination environment around Ni(II) in **2**.

A comparison of the various bond distance data among **1-6** (Table 3) clearly reveals the effect of

the lanthanide contraction for the Ln-O$_{phenolate}$ and for the Ln-O$_{OMe}$ bond distance (except Ni^{II}-

Ho[III]). Also, Ni-Ln distance sharply decreases from 3.443(12) to 3.395(14) Å from **1** to **6**. In this

context it is interesting to mention that the bond angle of Ni-O-Ln varies from 102.5° to 103. 4°

(**1-6**). In a system that is structurally close to the current examples, viz., [Ni(μ-L')(μ-

OAc)Dy(NO$_3$)$_2$] and [Ni(μ-L')(μ-NO$_3$)Dy(NO$_3$)$_2$]·2CH$_3$OH the Ni-O-Dy angles range from

101.4°-107. 4°.[19]

Table3. Important bond lengths (Å) and bond angles (°) parameter for complexes **1-5**.

Complex	Ni-N^a (Å)	Ni-O$^a_{phenolate}$ (Å)	Ln-O$^a_{phenolate}$ (Å)	Ln-O$^a_{OMe}$ (Å)	Ni-Ln (Å)	Ni-O-Ln^a (°)
Ni^{II}-Gd^{III}(**4**)	2.098(5)	2.043(4)	2.340(4)	2.574(5)	3.443(12)	103.32(4)
Ni^{II}-Tb^{III}(**2**)	2.101(6)	2.045(5)	2.325(5)	2.571(6)	3.425(1)	103.0(5)
Ni^{II}-Dy^{III}(**1**)	2.102(8)	2.045(7)	2.311(7)	2.568 (8)	3.404(1)	102.6(3)
Ni^{II}-Ho^{III}(**3**)	2.102(3)	2.046(3)	2.301(2)	2.572(3)	3.407(9)	103.06(5)
Ni^{II}-Er^{III}(**5**)	2.108(6)	2.042(6)	2.288(5)	2.560(6)	3.395 (14)	103.15(6)
Ni^{II}-Y^{III}(**6**)	2.096(3)	2.040(2)	2.289(2)	2.562(3)	3.393(11)	103.09(9)

^{a}average bond parameters.

All the complexes show intermolecular π-π [3.269(8) Å] interactions between two

cyclopentadienyl rings of two different ferrocene moieties (Figure 4) which are interestingly

absent in the ligand. Besides this, intermolecular hydrogen bonding (O-H---N) interaction is

present between the coordinated water of one molecule and the imine nitrogen of another [O13-

H13····N3*, 2.168(9) Å; O13-H1····N1*, 2.430(9) Å] (Figure 4). Conformational analysis of **1-6**

as well as the ligand H₂L reveals the presence of a *syn*-periplanar orientation for the two

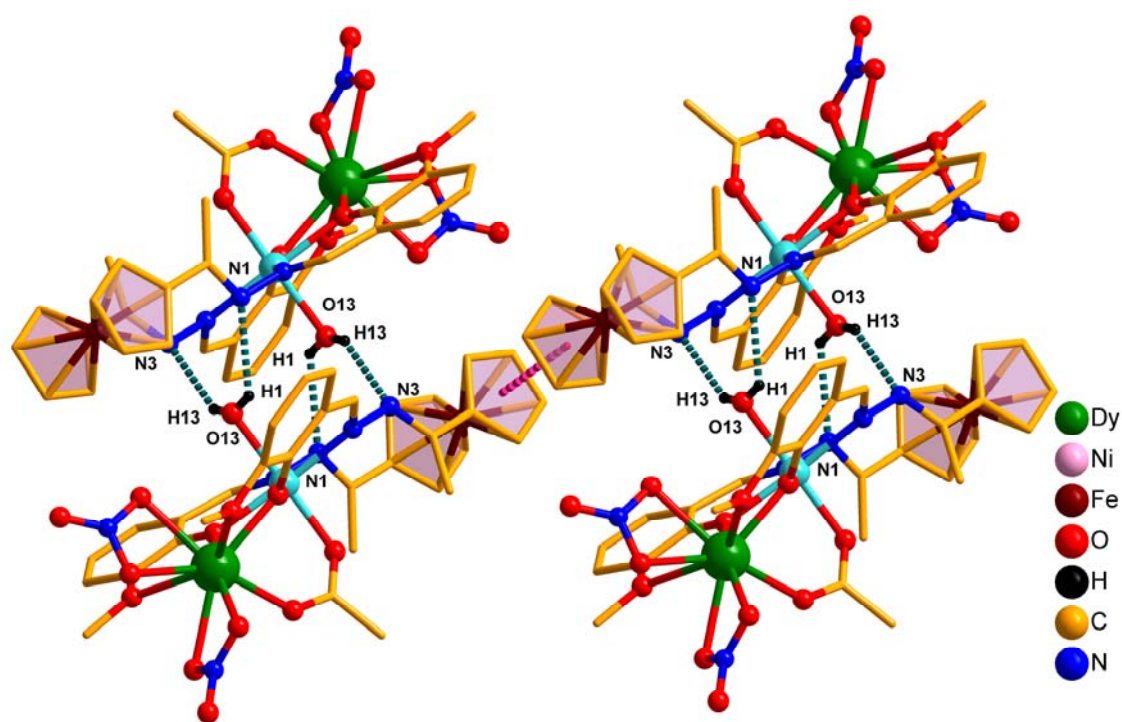cyclopentadienyl rings of the ferrocene moiety, with a torsion angle of ~3.2° (ESI).

Figure 4. View showing supramolecular hydrogen bonding and π···π stacking interactions in **1**.

Some hydrogen atoms have been omitted for the sake of clarity. The metric parameters involved

are (hydrogen bond distance) O13-H13····N3*, 2.168(9) Å; O13-H1····N1*, 2.430(9) Å; (bond

angle) O13-H13····N3*, 127.9(6)°;　O13-H1····N1*, 116.09(9)°; π···π, 3.269(8) Å. Symmetry

transformations used to generate equivalent atoms: x-1, y, z; −x, -y, -z.

Electrochemistry

Electrochemical properties of H_2L and **1-4** were studied by cyclic voltammetry (see Experimental Section). All the metal complexes (**1-4**) display nearly similar electrochemical behavior viz., two oxidative responses; one of these is reversible while the other is irreversible. The ligand on the other hand shows one quasi-reversible oxidative response (Figure 5; see also ESI).[14] The reversible/quasi reversible oxidative events for complexes **1-4** can be assigned to the ferrocene/ ferrocenium redox couple ($E_{1/2}$values ranging from 0.70 to 0.81 V, see Table 4).[14, 17] The irreversible oxidation event ($E_{1/2}$ values ranging from 1.31 to 1.44 V, see Table 4, see Figure 5 and ESI) is assigned to the Ni^{II}/Ni^{III} redox process.[20] The redox event of the ferrocene motif seems to be slightly different for the parent ligand vis-à-vis the complexes. Thus, the corresponding ΔEp in H_2L is larger in comparison to that observed in the metal complexes (Table 4). This may be due to two reasons. One as reported in the literature, complexation with transition metal ions improves the electronic communication in the ferrocene ring.[21] Secondly, in the free ligand, in the current instance, the redox-active hydrazone arms probably influence the ferrocene/ferrocenium couple. In the complexes, the electrons of the hydrazone arm are involved in binding to the metal ion. Consequently the redox response of the ferrocene motif in the complexes is more reversible (Table 4).The second oxidation potential values seem to be related to the incremental changes in Lewis acidity of the corresponding lanthanide ions. A systematic study correlating the influence of the redox inactive metal ion Lewis acidity on transition metal oxidation potentials has recently been published.[22]
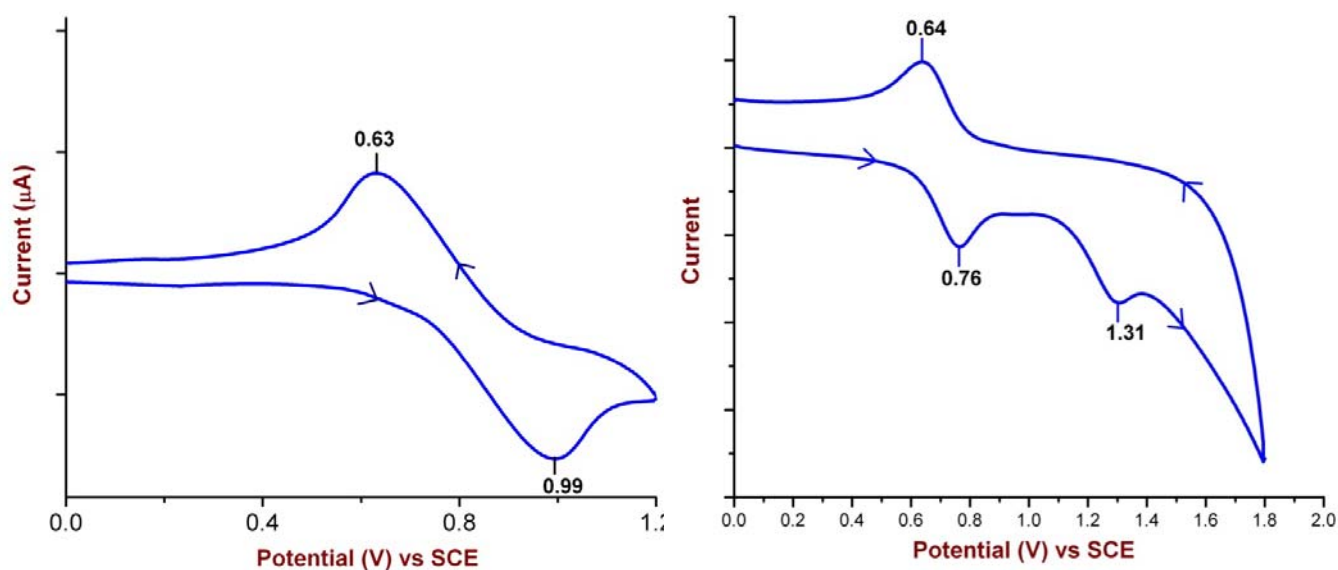
Figure 5. Cyclic voltammogram of (a) ligand(H_2L) and (b) [LNi(H_2O)(μ-OAc)Tb(NO_3)$_2$]· CH_3CN (**2**) in CH_2Cl_2 using glassy-carbon working electrode and TBAP as supporting electrolyte (scan rate 100mV/s).

Table 4. Electrochemical data for H_2L and the complexes **1-4**.

Compound	Oxidation(V)[a]	ΔE_p(mV)[b]	Oxidation (V)[c]
H_2L	0.81	360	-
1	0.79	100	1.38
2	0.70	120	1.31
3	0.80	120	1.44
4	0.78	120	1.34

[a]Half-wave potentials calculated from cyclic voltammetry as $E_{1/2} = (E_{p,a} + E_{p,c})/2$, peak[23] potential differences in mV in parentheses.

[b]ΔE_p, calculated from($E_{p,a}$- $E_{p,c}$); $E_{p,a}$: anodic peak potential, $E_{p,c}$: cathodic peak potential .[23]

[c]Peak potentials, $E_{p,a}$, for irreversible oxidation processes.

Magnetism behavior of compound 1-6

The *dc* magnetic behavior of compounds **1-6** was investigated using a SQUID magnetometer in the temperature range 2-300 K within a magnetic field of 1000 Oe and at T = 2 K in the magnetic field range of 0-6 Tesla. The powders were mulled in eicosane in order to prevent any orientation effect that may arise from the magnetic anisotropy of the compounds.

First, the magnetic properties of compound **6** (FeNiY) were investigated. Upon cooling from room temperature, $\chi_M T$ (1.1 $cm^3 mol^{-1} K$) is constant down to 40 K and then decreases to a value of 0.62 $cm^3 mol^{-1} K$ at T = 2 K (Figure 6). This is the expected behavior of a S = 1 (with g = 2.1) system with a zero-field splitting and/or weak intermolecular antiferromagnetic exchange coupling that are usually responsible of the decrease of $\chi_M T$ at low temperature. The magnetization *vs.* the magnetic field (0 - 5 T) was measured at three different temperatures (2, 4 and 6 K). The value at $\mu_0 H$ = 5 T and T = 2 K is equal to 1.76 BM, well below 2.1 expected for a S = 1 system with g = 2.1, which is the sign of the presence of a relatively large zero-field splitting (Figure 6, inset). The simultaneous best fit of the magnetization and the $\chi_M T$ data, performed using a home-made program, was obtained when considering a dimer of complexes. Indeed, the examination of the structure shows the presence of H-bonds between two neighboring molecules connecting the oxygen atoms of the apical water molecules linked to Ni^{II} to the nitrogen atoms of the other molecules, thus forming FeNiY dimers within the structure (Figure 4 and Figure S17) and no other H-bonds are present. In addition, π-π interactions between neighboring molecules are also present as shown in Figure 4. However, the Ni-Ni separation between two molecules having H-bonds is 5.5 Å, while this distance is 13.4 Å for molecules having π-π interactions. We will thus neglect the π interactions in the model used to

simulate the magnetic data. Based on the spin Hamiltonian $H = g\beta H_z -2J'S_{Ni1} \cdot S_{Ni2} + D[S_z^2 - S(S+1)/3]$, we obtain the following parameters g = 2.1, J' = - 0.1 cm^{-1} and D = - 7.8 cm^{-1} with an agreement factor of 2x10^{-5}, where J' is the exchange coupling between the Ni^{II} ions and D the axial zero-field splitting parameter. Trying to fit the data without considering the dimer model leads to a D value of - 8.9 cm^{-1} but the fit is of lower quality (agreement factor of 10^{-3}). Similarly, trying to impose a positive D value does not allow fitting simultaneously the χ_MT and the magnetization data. It is not possible to rationalize the sign of D without performing *ab initio* calculations, which is out of the scope of this paper but the magnitude can be understood considering the structural parameters (see below).
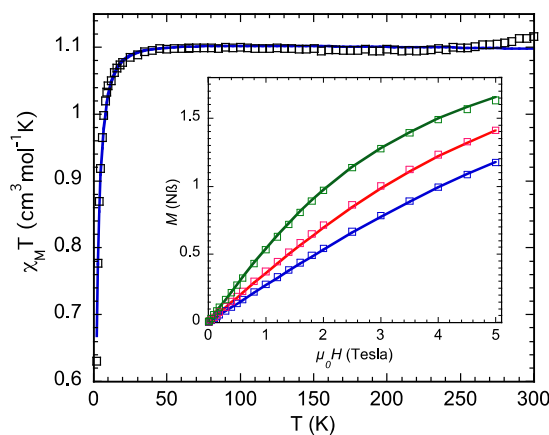

Figure 6. χ_MT = f(T) for **6** (experimental (□) and calculated (——) and M=f(μ_0H) ate T = 2 (blue), 4 (red) and 6 K (green).

For the FeNiGd complex (**4**), the χ_MT value at room temperature (9.01 cm^{3}mol^{-1}K) corresponds to the expected one for isolated Ni^{II} (S = 1, χ_MT = 1 cm^{3}mol^{-1}K for g = 2) and Gd^{III} (S = 7/2, χ_MT = 7.875 cm^{3}mol^{-1}K for g = 2) ions with an average 'g' value slightly larger than 2 (Figure 7). Upon cooling, χ_MT increases and reaches a maximum at of 11.09 cm^{3}mol^{-1}K at T = 5 K and then slightly decreases. The increase of χ_MT upon cooling is the signature of a ferromagnetic

exchange coupling between the Gd^{III} and the Ni^{II} through the oxygen bridges, which leads to a ground spin state S = 9/2. However, the largest $\chi_M T$ value (11.1 $cm^3mol^{-1}K$ at T = 5 K) is well below that expected for an S = 9/2 (17.875 $cm^3mol^{-1}K$ for an average g-value of 2). The relatively weak $\chi_M T$ value and its decrease below T = 5 K may be due to intermolecular antiferromagnetic interactions as in the case of the NiY complex and to the zero-field splitting of Ni^{II} since the anisotropy of Gd^{III} is very weak to induce such a large effect. The M = $f(\mu_0 H)$ plot (Figure 7, inset) at T = 2 K leads to value of 8.8 BM at $\mu_0 H$ = 6 T, lower than 9.1 expected for Ni^{II} (S = 1, g_{Ni} = 2.1) and Gd^{III} (S = 7/2 and g_{Gd} = 2.0). The $\chi_M T$ and the magnetization data were simultaneously fitted by the MAGPACK software[24], considering a dimer model as in the case of the NiY complex since the two compounds are isomorphous. Using the spin Hamiltonian (H = -$2JS_{Ni1} \cdot S_{Gd1}$ - $2JS_{Ni2} \cdot S_{Gd2}$ - $2J'S_{Ni1} \cdot S_{Ni2}$ + $D_{Ni}[S_z^2 - S(S+1)/3])$, the best fit leads to the following parameters: J = 0.77 cm^{-1}, J' = - 0.17 cm^{-1}, D_{Ni} = -7.8 cm^{-1} and g = 2.05 with an agreement factor of 2.5×10^{-5}. These data are in very good agreement with those obtained for the NiY complex and thus validate the sign and the magnitude of D and the presence of an intermolecular antiferromagnetic coupling between two adjacent molecules.
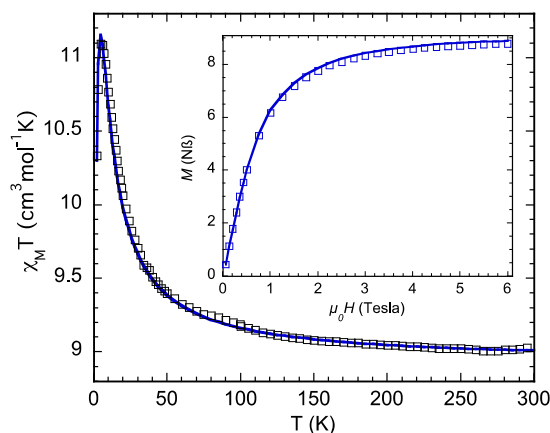
Figure 7. $\chi_M T = f(T)$ plot and $M = f(\mu_0 H)$ plot (inset) for **4** (experimental ($\square$) and calculated (—).

The zero-field splitting parameter is rather large for octahedral Ni^{II} complexes; |D| is usually hardly larger than 5 cm^{-1} when the coordination sphere is not very distorted.[25] On the other hand, , when a large distortion is present, particularly when one or two XNiX angles are far from 90° (either larger or weaker), a large magnetic anisotropy may be present.[7a,26] Here, the coordination sphere of Ni^{II} is rather distorted with two angles NNiN and ONiO equal to 104° and 80° respectively that may explain the large anisotropy that had to be considered to simulate the data. In conclusion, the experimental data show the presence of a ferromagnetic exchange coupling between the Ni^{II} and the Gd^{III} ions together with a weak intermolecular coupling ($J_{NiNi} \leq 0.1$ cm^{-1} and a non-negligible single ion axial zero-field splitting for Ni^{II} ($D_{Ni} \leq 10$ cm^{-1}). The ferromagnetic exchange coupling was already rationalized using theoretical calculations.[27] It is mainly the result of a charge transfer mechanism involving the 5d (and/or the 6s) orbitals of the lanthanide as in the case of the $Cu^{II}Gd^{III}$ complexes that were thoroughly studied.[28]

The $\chi_M T$ plots of the other four compounds **1**, **2**, **3** and **5** where Dy, Tb, Ho and Er replaced Gd are depicted in Figure 8. For all compounds, the $\chi_M T$ values at room temperature correspond to those expected for isolated Ni^{II} and Ln^{III} ions. Table 5 summarizes the calculated $\chi_M T$ values for the isolated ions and the experimental ones for the four complexes; we assume a g-value of 2.03 for Ni^{II} and thus a $\chi_M T$ value of 1.03 $cm^3 mol^{-1} K$ for Ni^{II} based of the results of the simulation of the NiGd data. The experimental data at high temperature are consistent with those expected from the isolated Ni^{II} and Ln^{III} ions.
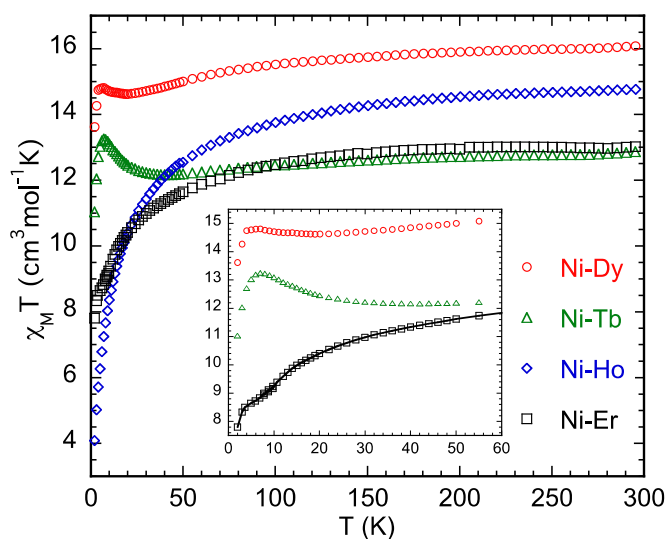

Figure 8. $\chi_M T = f(T)$ plots for compounds **1**(NiDy), **2**(NiTb), **3**(NiHo) and **5**(NiEr), the inset represents a zoom of the 0 – 60 temperature region.

Table 5. Theorertical g-values for the Ln^{III} ions and calculated and experimental $\chi_M T$ values for

1-**5** at room temperature.

Complex	$g_{Ln\ (=(L+2S)/J)}$	$\chi_M T$calculated for isolated ions	$\chi_M T$ experimental
NiGd **(4)**	2	8.9	9.01
NiDy **(1)**	4/3	15.2	16.0
NiTb **(2)**	3/2	12.9	12.8
NiHo **(3)**	5/4	15.1	14.8
NiEr **(5)**	6/5	12.5	12.9

The first qualitative observation concerns the general variation of $\chi_M T$ for the five compounds.

While for NiGd, $\chi_M T$ increases slightly upon cooling from room temperature $\chi_M T$ decreases for

the other complexes apart for the NiEr complex where $\chi_M T$ is almost constant between 300 and

150 K (Figure 8). This behavior is assigned, as it will be discussed below, to the depopulation of

the M_J sublevels of the ground J state of the lanthanides and not to an antiferromagnetic coupling

with Ni^{II} since apart from the Ho case a maximum of $\chi_M T$ is observed at low temperature.

For **1**, $\chi_M T$ decreases slightly upon cooling and reaches a minimum at T = 20 K. It, then, slightly

increases to a maximum at T = 5 K before decreasing at low temperature. This decrease of $\chi_M T$

from room temperature is due to the depopulation of the M_J sub-levels belonging to the J = 15/2

ground state (for Dy the ground spectroscopic state is $^{5/2}H_{15/2}$, S = 5/2, L = 5 and, because the f-

orbitals are more than half filled, J = 15/2). The slight increase below T = 20 K is the result of a ferromagnetic exchange coupling between Ni^{II} and Dy^{III} as for the NiGd complex. The behavior of complex **2** (NiTb) is similar indicating the presence of a ferromagnetic interaction between Ni^{II} and Tb^{III}. For complex **3** (NiHo), $\chi_M T$ decreases more quickly than for the other two complexes and, more importantly, no maximum of $\chi_M T$ is observed as for **1** and **2**. This behavior suggests the presence of an antiferromagnetic coupling in the NiHo complex. However, a ferromagnetic coupling cannot be excluded if a large depopulation of the M_J sub-levels occurs that may balance the weak increase of $\chi_M T$ due to the ferromagnetic coupling. For the Er-based complex **5**, $\chi_M T$ has a similar behavior to that of **3,** but here a slight leveling is observed between 10 and 7 K (Figure 8). Because the measurements were made using a weak magnetic field, because no saturation effects were observed under an applied field of 0.1 T and because the data are perfectly reproducible, the only explanation to the presence of a leveling is a ferromagnetic coupling between Er(III) and Ni(II) as for compounds **1**, **2** and **4**. Thus for the Er complex, the absence of a frank maximum for $\chi_M T$ is due to the depopulation of the M_J sub-levels as for the NiHo complex, but that does compensate the increase of $\chi_M T$ expected from the ferromagnetic exchange coupling between Ni^{II} and Er^{III}.

The magnetization data for **1**, **2**, **3** and **5** (Figure 9) correspond to those expected for each lanthanide ion considering at high field the addition of the signal due to Ni^{II}. Indeed, the magnetization values for the NiTb and NiHo (6.15 and 5.85 BM respectively at $\mu_0 H$ = 5 T and T = 2 K) correspond well to the experimental values of the ZnTb and ZnHo complexes already reported by some of us (4.5 and 4.3 BM at $\mu_0 H$ = 5 T and T = 2 K),[14] (see ESI, Figure S18) added to that corresponding to a Ni^{II} ion possessing a non-negligible magnetic anisotropy (around 1.6 BM at $\mu_0 H$ = 5 T and T = 2 K). Thus, the difference in the magnetization values

between the Zn and the Ni based complexes (at μ_0H = 5 T and T = 2 K) is compatible with the

magnetization of a Ni^{II} possessing an axial zero-field splitting |D| value in the range 5-10 cm^{-1}

considering the experimental and theoretical reported data on the magnetic anisotropy of

mononuclear Ni^{II} complexes. [7a-e, 25] This is in line with the value obtained from the simulation of

the M= f(H) and $\chi_M T$ = f(T) data of the NiGd complex (see above) and thus confirms the

presence of a non-negligible magnetic anisotropy on the Ni^{II} moiety even though it is not

possible to determine its nature (XY: positive D or Ising: negative D) and particularly the extent

of the rhombic contribution. Unfortunately, one cannot do the same comparison between the

NiDy and ZnDy complexes since the $\chi_M T$ value at room temperature and the magnetization

value of the already reported ZnDy complex are slightly lower than the expected one (see Figure

S18) as mentioned by the authors themselves.[14] For NiHo, the magnetization increases almost

continuously from 0 to 5 T, instead of increasing sharply for fields lower than 1 T and then

saturating above as usually observed for Ho^{III} complexes.[29] This behavior corresponds to that of

the mononuclear Ho^{III} within the ZnHo complex[14], where a monotonous increase of M upon

increasing the magnetic field was observed (see ESI, Figure S18). This is consistent with the low

temperature $\chi_M T$ data as due to a spectrum of the M_J sub-levels with energy separation small

enough so that the application of magnetic fields in the 0-5 Tesla range at T = 2 K leads to their

depopulation. One can thus conclude that for the Ho^{III} complex, the crystal field does not largely

lift the degeneracy of the J = 6 ground state and that a ferromagnetic exchange coupling cannot

be excluded despite the absence of a maximum in the $\chi_M T$ = f(T) curve (see discussion above).
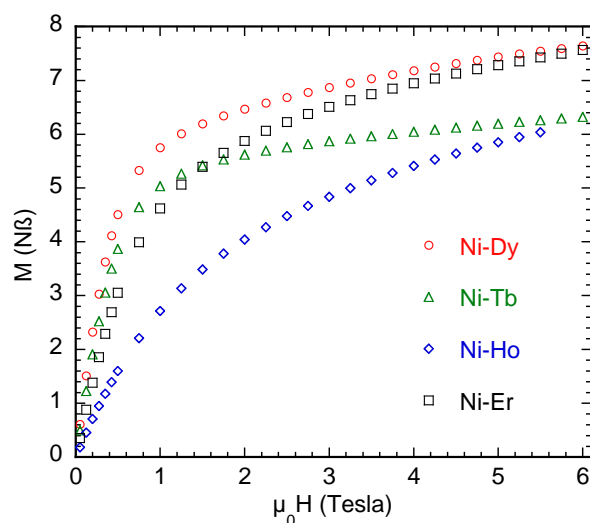
Figure 9. M = f(μ_0H) for compounds **1** (NiDy), **2** (NiTb), **3** (NiHo) and **5** (NiEr).

Even though it is not straightforward to simulate the χ_MT = f(T) data for **1-5**, the temperature of the maximum gives a rough idea on the relative magnitude of the exchange coupling parameters and a hint on the nature of the mechanism. The higher this temperature is, the larger is the ferromagnetic exchange interaction. The temperature values of the maximum of the χ_MT curves for NiGd, NiTb, NiDy and NiEr are 5, 5, 7 and 4 K respectively, while no maximum is observed for the NiHo complex. Apart from the case of Ho, it appears that the magnitude of the coupling does not dramatically change through the Ln^{III} series. If the exchange coupling interaction was due to the classical ferromagnetic mechanism of orthogonal orbitals (4f for the lanthanides and 3d for Ni^{II}), the magnitude of the coupling should decrease when going from Gd^{III} to Er^{III} because of the contraction of the f-orbitals. This is because the ferromagnetic contribution to the exchange coupling is related to the overlap density that is itself related to the extension of the magnetic orbitals through space. The experimental T$_{max}$ values (apart that of Ho^{III}) are in line with the mechanism that involves a charge transfer between the 4f and 5d orbitals where, a priori, the contraction of the f-orbitals has almost no effect on the magnitude of the coupling.

The dynamic magnetic susceptibilities were measured at different frequencies in the presence of

an oscillating magnetic field of 3 Oe for compounds **1**, **2** and **3** under zero *dc* field. No out-of-

phase (χ'') signals were observed above 2 K for the compounds as for the Zn analogues. The

application of a *dc* field of 1000 Oe allows the observation of an out of phase signals (χ'') for all

compounds but with maxima below T = 2 K (see ESI, Figure S19). Such behavior was absent in

the isostructural ZnLn complexes.[14] Thus, the replacement of the diamagnetic Zn^{II} by the

paramagnetic Ni^{II} that couples in a ferromagnetic manner to the Ln^{III} ions led to the appearance

of an out-of phase signal (with maxima of the $\chi'' = f(T)$ curves below 2 K) in the presence of an

applied *dc* magnetic field and thus to a field dependent slow relaxation of the magnetization.

Since the Zn and the Ni based complexes are isomorphous, the weak ferromagnetic coupling

between the two anisotropic Ni(II) and Ln(III) ions is responsible of the observed slow

relaxation. However, the presence of an antiferromagnetic exchange coupling between two

neighboring molecules within the compounds, even though very weak (J' = -0.17 cm^{-1}) leads to

an overall ground state S = 0 in zero field. This is probably responsible for the quantum

tunneling of the magnetization that does not allow observing the slow relaxation in the absence

of an applied dc field and at higher temperatures. Further studies on similar complexes with a

slightly modified bridging ligand in order to break the H-bonds that link the molecules will be

investigated. Furthermore, replacing Ni^{II} by Co^{II} and Cu^{II} will help to shed light on the origin of

slow relaxation in this family of complexes.

Conclusion

We have synthesized a new family of ferrocene-based dinuclear heterometallic Ni^{II}/ Ln^{III}

complexes $[LNi(H_2O)(\mu\text{-}OAc)Ln(NO_3)_2$. CH_3CN; Ln= Dy^{III}(**1**), Tb^{III}(**2**), Ho^{III}(**3**), Gd^{III}(**4**),

Er^{III}(**5**), Y^{III}(**6**)] . The synthesis of **1-6** was accomplished by using dual compartmental ligand based on ferrocene scaffold. Magnetic measurements of **1-6** reveal that below 50K the χ_MT product of the complexes Ni^{II}/ Dy^{III} (**1**), Ni^{II}/Tb^{III} (**2**), Ni^{II}/ Gd^{III} (**4**), and Ni^{II}/Er^{III} (**5**) slowly increases, showing a ferromagnetic exchange coupling between Ni^{II} and Ln^{III} centers. On the other hand the χ_MT product of the Ni^{II}/Ho^{III} (**3**) complex does not exhibit a maximum. However the presence of a ferromagnetic coupling cannot be excluded and it is assumed that the depopulation of the M_J sub-levels is responsible of the absence of the maximum based of the shape of the magnetization *vs.* field at T=2 K. We have further synthesized Ni^{II} /Y^{III} (**6**) complex in order to investigate the amount of anisotropy present in Ni^{II} ion. AC susceptibility measurement at various frequencies reveal that an out-of-phase (χ'') signal was observed, upon the application of 1000 Oe *dc* field but no maxima was observed above T= 2 K. This is attributed to the weak exchange coupling between the Ni^{II} and Ln^{III} ions that was absent in the previously reported Zn^{II}Ln^{III} complexes.[14] However, the presence of the antiferromagnetic coupling between two neighboring molecules precludes the observation of the slow relaxation at higher temperatures.

In conclusion a dual compartmental ligand H$_2$L constructed on a ferrocene scaffold has been successfully used to prepare neutral dinuclear heterometallic Ni^{II}/ Ln^{III} complexes that exhibit a slow relaxation of the magnetization albeit at very low temperataure. The ferrocene-based ligand appears to be versatile enough to allow the assembly of other 3d/4f metal assemblies. We are currently focusing on the Co^{II}/Ln^{III} and Cu^{II}/Ln^{III} complexes in order to examine the effect of the paramagnetic transition metal ions and the 3d-4f exchange coupling on the slow relaxation processes in this family of complexes.

Electronic Supplementary Information (ESI). Crystallographic information files (CIF), CCDC 993944-993949 for **1-6**., Tables of bond distance (**Å**) and bond angle (˚), details of ESI-MS(**1-6**), electrochemistry studies of compounds **1-4,** UV-Vis spectra of **1-6,** and additional figures.

References

1. a) M. Andruh, *Chem. Commun.,* 2011, **47**, 3025; (b) V. Chandrasekhar and B. M. Pandian, *Acc. Chem. Res.,* 2009, **42**, 1047; (c) M. Andruh, J.-P. Costes, C. Diaz and S. Gao, *Inorg. Chem.,* 2009, **48**, 3342; (d) S. Akine, T. Taniguchi and T. Nabeshima, *J. Am. Chem. Soc.,* 2006, **128**, 15765.

2. (a) W. K. Wong, H. Liang, W. Y. Wong, Z. Cai, K. F. Li and K. W. Cheah, *New J. Chem.,* 2002, **26**, 275; (b) O. M. P. G. Lacroix, J.-P. Costes, B. Donnadieu, C. Lepetit, and K. Nakatani, *Inorg. Chem.,* 2004, **43**, 4743; (c) J. An, C. M. Shade, D. A. Chengelis-Czegan, S. Petoud and N. L. Rosi, *J. Am. Chem. Soc.*, 2011, **133**, 1220; (d) X. Yang, R. A. Jones, V. Lynch, M. M. Oye, A. L. Holmes, *Dalton Trans.,* 2005, 849.

3.(a) V. Chandrasekhar, A. Dey, S. Das, M. Rouzières and R. Clérac, *Inorg. Chem.,* 2013, **52**, 2588; (b) G. Novitchi, W. Wernsdorfer, L. F. Chibotaru, J.-P. Costes, C. E. Anson and A. K. Powell, *Angew. Chem., Int. Ed*., 2009, **48**, 1614; (c) S. K. Langley, L. Ungur, N. F. Chilton, B. Moubaraki, L. F. Chibotaru and K. S. Murray, *Chem. Eur. J*., 2011, **17**, 9209; (d) H. L. C. Feltham, R. Clérac, L. Ungur, L. F. Chibotaru, A. K. Powell and S. Brooker, *Inorg. Chem.,* 2013, **52**, 3236; (e) S. Osa, T. Kido, N. Matsumoto, N. Re, A. Pochaba, and J. Mrozinski, *J. Am. Chem. Soc*., 2004, **126**, 420; (f) V. Baskar, K. Gopal, M. Helliwell, F. Tuna, W. Wernsdorfer, and R. E. P. Winpenny, *Dalton Trans*., 2010, **39**, 4747.

4. (a) A. Mishra, W. Wernsdorfer, S. Parson, G. Christou and E. Brechin, *Chem. Commun.,* 2005, 2086; (b) A. Saha, M. Thompson, K. A. Abboud, W. Wernsdorfer and G. Christou, *Inorg. Chem*., 2011, **50**, 10476; (c) V. Chandrasekhar, P. Bag, M. Speldrich, J. V. Leusen and P. Kögerler, *Inorg.Chem*., 2013, **52**, 5035; (d) T. Shiga, T. Onuki, T. Matsumoto, H. Nojiri, G.N. Newton, N. Hoshinoa and H. Oshio, *Chem. Commun.,* 2009, 3568. (e) M. N. Akhtar, Y.-Z. Zheng, Y. Lan, V. Mereacre, C. E. Anson and A. K. Powell, *Inorg. Chem.,* 2009, **48**, 3502; (f) H. Ke, L. Zhao, Y. Guoa and J. Tang, *Dalton Trans.,* 2012, **41**, 2314; (g) C. Papatriantafyllopoulou, K. A. Abboud and G. Christou, *Inorg. Chem.,* 2011, **50**, 8959; (h) M. Holynska, D. Premuzic, I.-R. Jeon, W. Wernsdorfer, R. Clérac and S. Dehnen, *Chem. Eur. J.,* 2011, **17**, 9605.

5.(a) A. K. Boudalis, Y. Sanakis, J. M. Clemente-Juan, B. Donnadieu, V. Nastopoulos, A. Mari, Y. Coppel, J. P. Tuchagues and S. P. Perlepes, *Chem. Eur. J.,* 2008, **14**, 2514; (b) D. E. Freedman, W. H. Harman, T. D. Harris, G. J. Long, C. J. Chang and J. R. Long, *J. Am. Chem. Soc.,* 2010, **132**, 1224; (c) A. Baniodeh, I. J. Hewitt, V. Mereacre, Y. Lan, G. Novitchi, C. E. Anson and A. K. Powell, *Dalton Trans.,* 2011, **40**, 4080; (d) A. M. Ako, V. Mereacre, Y. H. Lan, W. Wernsdorfer, R. Clérac, C. E. Anson and A. K. Powell, *Inorg. Chem.,* 2010, **49**, 1; (e) N.

Hoshino, A. M. Ako, A. K. Powell and H. Oshio, *Inorg. Chem*., 2009, **48**, 3396; (f) S. Mossin, B. L. Tran, D. Adhikari, M. Pink, F. W. Heinemann, J. Sutter, R. K. Szilagyi, K. Meyer and D. J. Mindiola, *J. Am. Chem. Soc.,* 2012, **134**, 13651; (g) R. Bagai, W. Wernsdorfer, K. A. Abboud and G. Christou, *J. Am. Chem. Soc*., 2007, **129**, 12918; (h) M. Ferbinteanu, T. Kajiwara, K.-Y. Choi, H. Nojiri, A. Nakamoto, N. Kojima, F. Cimpoesu, Y. Fujimura, S. Takaishi and M. Yamashita, *J. Am. Chem. Soc.,* 2006, **128**, 9008.

6. (a) O. Roubeau and R. Clérac, *Eur. J. Inorg. Chem*., 2008, 4325. (b) D. Gatteschi, R. Sessoli, and J. Villain, *Molecular Nanomagnets;* Oxford University Press: Oxford, U.K., 2006**.**

7. (a) G. Rogez, J. N. Rebilly, A. L. Barra, L. Sorace, G. Blondin, N. Kirchner, M. Duran, J. van Slageren, S. Parsons, L. Ricard, A. Marvilliers and T. Mallah, *Angew. Chem. Int. Ed.* 2005, **44**, 1876 ; (b) J. N. Rebilly, G. Charron, E. Riviere, R. Guillot, A. L. Barra, M. D. Serrano, J. van Slageren and T. Mallah, *Chem. Eur. J.* 2008, **14**, 1169. (c) J. M. Zadrozny and J. R. Long, *J. Am. Chem. Soc.,* 2011, **133**, 20732 ; (d) R. Ruamps, L. J. Batchelor, R. Maurice, N. Gogoi, P. Jiménez-Lozano, N. Guihéry, C. de Graaf, A.-L. Barra, J.-P. Sutter and T. Mallah, *Chem. Eur. J.* 2013, **19**, 950 ; (e) R. Ruamps, R. Maurice, L. Batchelor, M. Boggio-Pasqua, R. Guillot, A. L. Barra, J. Liu, E. E. Bendeif, S. Pillet, S. Hill, T. Mallah and N. Guihéry, *J. Am. Chem. Soc.,* 2013, **135**, 3017 ; (f) S. Gomez-Coca, E. Cremades, N. Aliaga-Alcalde and E. Ruiz, *J. Am. Chem. Soc.,* 2013, **135**, 7010.

8. (a) G. J. Sopasis, M. Orfanoudaki, P. Zarmpas, A. Philippidis, M. Siczek, T. Lis, J. R. O'Brien and C. J. Milios, *Inorg. Chem.,* 2012, **51**, 1170; (b) M. Ibrahim, Y. Lan, B. S. Bassil, Y. Xiang, A. Suchopar, A. K. Powell and U. Kortz, *Angew. Chem., Int. Ed.,* 2011, **50**, 4708; (c) M. H. Zeng, M. X. Yao, H. Liang, W. X. Zhang and X. M. Chen, *Angew. Chem., Int. Ed.* **2007**, *46*,

1832; (d) S. K. Langley, N. F. Chilton, L. Ungur, B. Moubaraki, L. F. Chibotaru and K. S. Murray, *Inorg. Chem.,* 2012, **51**, 11873; (e) K. W. Galloway, A. M. Whyte, W. Wernsdorfer, J. Sanchez-Benitez, K. V. Kamenev, A. Parkin, R. D. Peacock and M. Murrie, *Inorg. Chem.*, 2008, **47**, 7438; (g) M. Murrie, *Chem. Soc. Rev.* 2010, **39**, 1986; (h) T. Yamaguchi, J.-P. Costes, Y. Kishima, M. Kojima, Y. Sunatsuki, N. Bréfuel, J.-P. Tuchagues, L. Vendier, and W. Wernsdorfer, *Inorg. Chem.,* 2010, **49**, 9125; (i) L. Ungur, M. Thewissen, J.-P. Costes, W. Wernsdorfer, and L. F. Chibotaru, *Inorg. Chem.,* 2013, **52**, 6328; (j) J.-P. Costes, Laure Vendiera, and W. Wernsdorfer, *Dalton Trans.*, 2011, **40**, 1700.

9. (a) S. M. T. Abtab, M. Maity, K. Bhattacharya, E. C. Sañudo and M. Chaudhury, *Inorg. Chem.* 2012, **51**, 10211; b) M. A. Palacios, A. J. Mota, J. Ruiz, M. M. Hänninen, R. Sillanpää and E. Colacio *Inorg. Chem.*, 2012, **51**, 7010; (c) T. D. Pasatoiu, J.-P. Sutter, A. M. Madalan, F. Z. C. Fellah, C. Duhayon and M. Andruh, *Inorg.Chem.* 2011, **50**, 5890; (d) G. Cosquer, F. Pointillart, B. L. Guennic, Y. L. Gal, S. Golhen, O. Cador and Ouahab, L. *Inorg. Chem.,* 2012, **51**, 8488; (e) E. Colacio, J. Ruiz, A. J. Mota, M. A. Palacios, E. Cremades, E. Ruiz, F. J. White and E. K. Brechin, *Inorg. Chem.,* 2012, **51**, 5857.

10. (a) V. Chandrasekhar, B. M. Pandian, J. J. Vittal and R. Clérac, *Inorg. Chem.,* 2009, **48**, 1148; (b) V. Chandrasekhar, B. M. Pandian, R. Boomishankar, A. Steiner, J. J. Vittal, A. Houri and R. Clérac, *Inorg. Chem.,* 2008, **47**, 4918; (c) V. Chandrasekhar, B. M. Pandian, R. Azhakar, J. J. Vittal and R. Clérac, *Inorg. Chem.,* 2007, **46**, 5140.

11. V. Chandrasekhar, T. Senapati, A. Dey, S. Das, M. Kalisz and R. Clérac, *Inorg. Chem.,* 2012, **51**, 2031.

12. (a) P. Štěpnička, Eds.; *Ferrocenes: Ligands, Materials and Biomolecules*; John Wiley and Sons. Ltd., Chichester, 2008; (b) A. Togni and T. Hayashi, Eds.; *Ferrocenes*; VCH Publishers: Weinheim, Germany, 1995; (c) R. G. Arrayás, J. Adrio and J. C. Carretero, *Angew. Chem. Int. Ed.*, 2006, **45**, 7674; (d) G. Bandoli and A. Dolmella, *Coord. Chem. Rev.* 2000**, 209**, 161; (e) T. J. Colacot, *Chem. Rev.,* 2003, **103**, 3101;　(f) R. C. J. Atkinson, V. C. Gibson and N. J. Long, *Chem. Soc. Rev.*, 2004, **33**, 313.

13. (a) O. Kahn, J. Galy, Y. Journaux, J. Jaud and I. Morgenstern Badarau, *J. Am. Chem. Soc.*, 1982**, 104**, 2165; (b) Y. Journaux, O. Kahn, J. Zarembowitch, J. Galy and J. Jaud, *J. Am. Chem. Soc.* 1983**, 105**, 7585.

14. V. Chandrasekhar, A. Chakraborty and E. C. Sañudo, *Dalton Trans*. 2013, **42**, 13436.

15. (a) B. S. Furniss, A. J. Hannaford, P. W. G. Smith and A. R. Tatchell, *Vogel's Text Book of Practical Organic Chemistry,* 5th ed., ELBS, Longman: London, 1989; (b) D. B. G. Williams and M. Lawton, *J. Org. Chem.*2010, **75**, 8351.

16. D. Zhang, Q. Zhang, J. Sua and H. Tian, *Chem. Commun*. 2009, 1700.

17. F. Chen-jie, D. Chun-ying, M. Hong, H. Cheng, M. Qing-jin, L. Yong-jiang, M. Yu-hua and W. Zhe-ming, *Organometallics,* 2001**, 20***,* 2525.

18. (a) *SMART & SAINT Software Reference manuals*, Version 6.45; Bruker Analytical X-ray Systems, Inc.: Madison, WI, 2003; (b) G. M. Sheldrick, SADABS*, a software for empirical absorption correction*, Ver. 2.05; University of Göttingen: Göttingen, Germany, 2002; (c) *SHELXTL, Reference Manual*, Ver. 6.1; Bruker Analytical X-ray Systems, Inc.: Madison, WI, 2000; (d) G. M. Sheldrick, *SHELXTL*, Ver. 6.12; Bruker AXS Inc.: Madison, WI, 2001; (e) Sheldrick, G. M. SHELXL97, *Program for Crystal Structure Refinement*; University of

Göttingen: Göttingen, Germany, 1997. (f) K. Bradenburg, *Diamond, Ver. 3.1eM*; Crystal Impact GbR: Bonn, Germany, 2005**.**

19. E. Colacio, J. e Ruiz-Sanchez, F. J. White and E. K. Brechin, *Inorg. Chem.,* 2011, **50**, 7268.

20. (a) S. Mandal, V. Balamurugan, F. Lloret and R. Mukherjee, *Inorg. Chem.,* 2009, **48**, 7544; (b) K. S. Bharathi, S. Sreedaran, A. K. Rahiman and V. Narayanan, *Spectrochim. Acta Part A*, 2013**, 105**, 245; (c) S. Pandey, P. P. Das, A. K. Singh and R. Mukherjee, *Dalton Trans.*, 2011, **40**, 10758; (d) T. J. Hubin, N. Tyryshkin, N. W. Alcock and D. H. Busch, *Acta Cryst.,* 2001,**C57**, 359; (e) V. V. Pavlishchuk, S. V. Kolotilov, A. W.; Addison, R. J. Butcher and E. Sinn, *Dalton Trans.*, 2000, 335.

21. N. Sadhukhan and J. K. Bera, *Inorg. Chem.,* 2009, **48**, 978.

22. E. Y. Tsui and T. Agapie, *Proc. Natl. Acad. Sci. U.S.A.***,**2013, doi/10.1073/pnas.1302677110.

23. J. Heinze, *Angew. Chem. Int. Ed. Engl*. 1984, **23***,* 831.

24. J. J. Borrás-Almenar, J. M. Clemente-Juan, E. Coronado, B. S. Tsukerblat, *J. Comput. Chem.,* 2001, **22**, 985.

25. (a) J. N. Rebilly, L. Catala, G. Charron, G. Rogez, E. Rivière, R. Guillot, P. Thuéry, A. L. Barra and T. Mallah, *Dalton Trans.,* 2006, 2818 ; (b) G. Charron, F. Bellot, F. Cisnetti, G. Pelosi, J. N. Rebilly, E. Rivière, A. L. Barra, T. Mallah and C. Policar, *Chem. Eur. J.,* 2007, **13**, 2774**.**

26. R. Maurice, R. Bastardis, C. de Graaf, N. Suaud, T. Mallah and N. Guihéry, *J. Chem. Th. Comput.,* 2009, **5**, 2977.

27. S. K. Singh, N. K. Tibrewal and G. Rajaraman, *Dalton Trans.,* 2011, **40**, 10897.

28. (a) O. Kahn, *Angew Chem. Int. Ed.,* 1985, **24**, 834; (b) J. Paulovic, F. Cimpoesu, M. Ferbinteanu and K. Hirao, *J. Am. Chem. Soc.,* 2004, **126**, 3321. (c) G. Rajaraman, F. Totti, A. Bencini, A. Caneschi, R. Sessoli and D. Gatteschi, *Dalton Trans.,* 2009, 3153; (c) J. P. Costes, T. Yamaguchi, M. Kojima and L. Vendier, *Inorg.Chem.,* 2009, **48**, 5555.

29. V. E. Campbell, R. Guillot, E. Rivière, P. T. Brun, W. Wernsdorfer and T. Mallah, *Inorg. Chem.,* 2013, **52**, 5194.

A Ferrocene-based Ligand for the Assembly of Heterobimetallic Ni[II]-Ln[III] (Ln[III] = Dy[III], Tb[III], Gd[III],Ho[III], Er[III], Y[III]) Complexes: Slow Relaxation of the Magnetization in Dy[III,] Tb[III] and Ho[III] Analogues

Amit Chakraborty,[a] Prasenjit Bag,[a] Eric Rivière,[b] Talal Mallah[b], Vadapalli Chandrasekhar[a,c]

[a]Department of Chemistry, Indian Institute of Technology Kanpur, Kanpur-208016, India;

[b]Institut de Chimie Moleculaire et Mate riaux d'Orsay, Universite Paris-Sud 11, F-91405, Orsay, France.

[c]National Institute of Science Education and Research, Institute of Physics Campus, Sachivalaya Marg, Sainik School Road, Bhubaneshwar-751 005, Odisha, India;

AUTHOR EMAIL ADDRESS: vc@iitk.ac.in,

talal.mallah@gmail.com